Exploiting Digital Micro-Mirror Devices for Ambient Light Communication

Xu, Talia; Tapia, Miguel Chávez; Zúñiga, Marco

Exploiting Digital Micro-Mirror Devices
for Ambient Light Communication

Talia Xu, Miguel Chávez Tapia, and Marco Zúñiga, *Technical University Delft*

https://www.usenix.org/conference/nsdi22/presentation/xu-talia

This paper is included in the Proceedings of the
19th USENIX Symposium on Networked Systems
Design and Implementation.

April 4–6, 2022 • Renton, WA, USA

978-1-939133-27-4

Open access to the Proceedings of the
19th USENIX Symposium on Networked
Systems Design and Implementation
is sponsored by

Exploiting Digital Micro-Mirror Devices for Ambient Light Communication

Talia Xu, Miguel Chávez Tapia, and Marco Zúñiga

Technical University Delft

{m.xu-2, m.a.chaveztapia, m.a.zunigazamalloa}@tudelft.nl

Abstract

There is a growing interest in exploiting *ambient light* for wireless communication. This new research area has two key advantages: it utilizes a free portion of the spectrum and does not require modifications of the lighting infrastructure. Most existing designs, however, rely on a single type of optical surface at the transmitter: liquid crystal shutters (LCs). LCs have two inherent limitations, they cut the optical power in half, which affects the range; and they have slow time responses, which affects the data rate. We take a step back to provide a new perspective for ambient light communication with two novel contributions. First, we propose an optical model to understand the fundamental limits and opportunities of ambient light communication. Second, based on the insights of our analytical model, we build a novel platform, dubbed PhotoLink, that exploits a different type of optical surface: digital micro-mirror devices (DMDs). Considering the same scenario in terms of surface area and ambient light conditions, we benchmark the performance of PhotoLink using two types of receivers, one optimized for LCs and the other for DMDs. In both cases, PhotoLink outperforms the data rate of equivalent LC-transmitters by factors of 30 and 80: 30 kbps & 80 kbps vs. 1 kbps, while consuming less than 50 mW. Even when compared to a more sophisticated multi-cell LC platform, which has a surface area that is 500 times bigger than ours, PhotoLink's data rate is 10-fold: 80 kbps vs. 8 kbps. To the best of our knowledge this is the first work providing an optical model for ambient light communication and breaking the 10 kbps barrier for these types of links.

1 Introduction

In the last two decades, the adoption of wireless communication has gone through an unprecedented expansion. This ever-increasing demand has raised warnings of a looming 'radio frequency (RF) crisis' [5], and various alternative technologies are being explored to mitigate this risk. Among them, visible light communication (VLC) has gained significant attention due to its wide, free and unregulated spectrum. VLC is a sub-area of optical wireless communication (OWC) that focuses on light sources that are incoherent, divergent and multichromatic (such as sunlight and artificial white light). VLC allows standard LEDs to provide illumination and communication and it is enabling several novel applications, from interactive toys [23], indoor positioning systems [27], to LiFi [20]. VLC, however, has an important limitation: it requires direct (*active*) control over the circuitry of the light source to modulate its intensity. Most of the light in our environments comes from sources we cannot control directly, not only the sun but also plenty of artificial lighting.

To exploit the vast presence of *ambient light*, researchers are investigating backscattering (*passive*) communication. Passive-VLC modulates ambient light using liquid crystal shutters (LCs). LCs can be seen as light shutters that allow (or block) the passage of light to communicate logical ones (or zeros). Recent studies report ambient light links reaching more than 50 m with data rates around 1 kbps, while consuming only a few mWs [7, 25]. Ambient light communication is a transformative eco-friendly concept because it piggybacks on top of energy that already exists, but current passive-VLC studies face two main challenges.

Challenge 1: *There has been no optical analysis of various passive VLC systems.* In a way, our community has rushed into the design of systems without carrying out first a proper optical analysis of the various types of ambient light and their impact on communication. Hence, several designs have been implemented reporting a wide range of *(i)* coverages (from a few meters to several tens of meters), *(ii)* data rates (from hundreds of bps to several kbps), and *(iii)* lighting conditions (from cloudy and sunny days to various types of artificial lighting). However, without an analytical framework, it is difficult to define a common baseline to directly compare and understand which elements contribute to such disparate performance. More importantly, we cannot provide insights about the fundamental opportunities and limits of ambient light communication.

Challenge 2: *Transmitters focus on a single optical device.* State-of-the-art (SoA) designs in passive VLC studies have been mainly constrained to a single type of optical surface,

the LCs, but LCs have some inherent limitations. First, even before any type of modulation begins, LCs cut the optical power in half due to the use of polarizers. This undesirable, but necessary, property of LCs reduces the communication range. Second, LCs have inherently slow rise and fall times, which has limited the data rate of all *single-cell* designs to values around 1 kbps [7, 13, 29]. Our design space could broaden greatly if we include other types of optical surfaces.

In this work, we take a step back to rethink passive-VLC. First, we propose a simple optical model to gain fundamental insights. Then, based on the outcomes of our model, we explore the use of digital micromirror devices (DMDs), which have different operating principles compared to LCs. In particular, our work makes the following contributions:

Contribution 1 [section 2]: An optical model for ambient light communication. Our model includes a key optical principle that has not been considered in ambient light communication: the fact that the performance depends not only on the luminous flux of the light source (output power) but also on its radiation pattern (diffused or directional). For example, this insight explains why a system tested under artificial light can perform better than under diffuse sunlight, even though diffuse sunlight can provide illumination that is an order of magnitude higher than artificial lighting.

Contribution 2 [section 3]: A new type of transmitter device. Our model shows that maintaining directional light patterns is central for passive links, but maintaining such directionality requires the right type of *(i)* ambient light and *(ii)* transmitter (optical surfaces with specular reflection). To attain that goal, we propose a novel transmitter based on DMDs. Inexpensive DMDs, however, are designed for video projection and provide slow update rates, around a few hundred Hz. We design a custom controller to generate carriers up to 220 kHz. Our novel transmitter provides higher contrast and faster switching speed, allowing us to increase the data rate of passive links by a factor of 80 compared to LC transmitters.

Contribution 3 [section 4 and section 5]: An implementation and thorough evaluation of our platform. We build two transmitters, one with a DMD and the other with an LC; and two receivers, one optimized for LCs and the other for DMDs. Using the same setup for all evaluations, in terms of surface area and illumination, our results show that (i) if we use the receiver optimized for LCs, PhotoLink attains 30 kbps for a distance of six meters and a BER below 1%, compared to the 1 kbps provided by the LC for the same range and BER [3, 7, 29], (ii) if we use the receiver optimized for DMDs, the data rate increases to 80 kbps. This performance is obtained with a power consumption around 45 mW. Furthermore, even if we compare PhotoLink with a *multi-cell* LC system having a surface area that is 500+ times bigger than ours (66 cm^2 vs. 0.13 cm^2) [28], PhotoLink can achieve an order of magnitude higher data rate (80 kbps vs. 8 kbps). To the best of our knowledge, our work is the first to break the 10 kbps barrier with ambient light communication.

2 System Analysis

A passive VLC system has three basic components, the emitter (light source), the transmitter (modulating surface) and the receiver. Every SoA study adopts a different set of components. Some studies use a light bulb as the emitter, others use a flashlight or the sun. Some studies use a diffuser at the modulating surface, others use retro-reflectors or aluminium plates. Some studies use lenses at the receivers, others do not. This wide range of set ups is, in part, responsible for the equally wide range of performances reported in the literature, with data rates ranging from 0.5 kbps to 8.0 kbps to link distances ranging from 2 m to 80 m [3, 13, 25, 26, 28, 29].

Leaving aside the specific modulation methods of all these studies, we want to gain a fundamental understanding of passive systems and their components. Building upon the models developed for free-space optics [21], we propose a framework to analyze passive communication with ambient light.

2.1 Maintaining the luminous flux

First, let us start with a guideline that, to the best of our knowledge, has not been stated in any prior passive-VLC study: *The most important aim in passive communication is to convey as much* LUMINOUS FLUX *as possible from the emitter to the receiver*. The *luminous flux*, which is measured in *lumen*, is different from *illuminance*, which is measured in *lux* (lux = lumen per unit area). To compare two different systems fairly, one should know at least the area and the illuminance at the transmitter (modulating surface). This represents the amount of energy that is captured by the transmitter (E_C). Unfortunately, few studies report these two pieces of information.

The luminous flux, however, is not the only important parameter. Equally important is the radiation pattern, which determines how much luminous flux is maintained throughout the optical link (i.e., how much of E_C is able to arrive at the receiver). To highlight the importance of the radiation pattern, Fig. 2 depicts a *specular (mirror-like)* surface under four different types of light sources. The effect on the luminous flux is shown from more to less directive:

a) Ideal. First, to exemplify an ideal setup, let us use a laser, which is a highly directional source where the luminous flux is hardly lost. Due to this property, lasers are used extensively for long-distance free-space communication. Lasers, however, are a fundamentally different type of light source that is not as pervasive (or safe) as natural or artificial white light, and therefore, it is considered only as a reference in this paper.

b) Directional (sunlight in a clear day). On a clear day, sunlight rays travel in parallel and a specular surface maintains that directionality (luminous flux) towards the receiver. *We found only one study exploiting this setup, but with LCs [7]. Our platform shows the significant gains that can be obtained in this setup using DMDs.*

c) Lambertian (light bulbs and flashligths). With light bulbs, only a fraction of the luminous flux radiated by the source reaches the surface (green arrows in Fig. 1c). Further-

(a) Ideal
[laser]

(b) Directional
[direct sunlight]

(c) Lambertian
[light bulb]
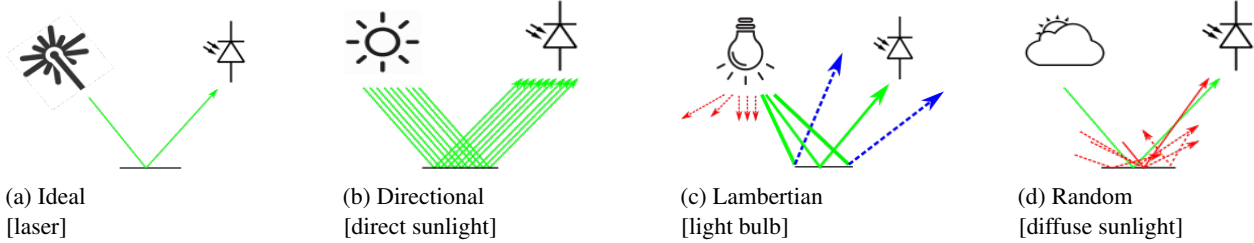
(d) Random
[diffuse sunlight]

Figure 1: The effect of different radiation patterns on the luminous flux. The reflective surface is specular.

more, since rays are radiated in different angles, when the luminous flux hits the surface, some rays are lost because the impinging angle is either too broad or too narrow to hit the receiver (blue arrows). *This scenario is used by all the backscattering studies reported in the literature [13, 25, 28, 29].*

d) Random (sunlight in a cloudy day). Clouds scatter sunlight, emitting rays uniformly in random directions. Due to this phenomenon, only an infinitesimally small fraction of the rays will impinge the surface at the right angle to reach the receiver (green arrow in Fig. 1d). *Our model shows that this is the worst case scenario with specular surfaces. No practical links can be obtained in this setup.*

The key point of this preliminary analysis is to highlight the importance of maintaining the luminous flux throughout the optical link. In the next subsection, we present a model to capture more detailed insights with a ray-tracing simulator.

2.2 Ray-tracing model

A 2D representation of a typical passive system is shown in Fig. 2a. The optical link has two main parts. *First*, the link between emitter and transmitter. Light is emitted from the light source O_L, with a (yellow) wavefront represented by A_L. The modulating surface O_T, acting as a transmitter, is at a distance D_{LT} from the light source, and receives a fraction of the luminous flux emitted by O_L. *Second*, the link between transmitter and receiver. The flux reflected by the surface O_T is represented with a (blue) wavefront A_T[1]. The photoreceiver O_R is at a distance D_{TR} from the transmitter, and collects only a fraction of the flux reflected by O_T. Another relevant parameter is the Field-of-View (FoV) of the receiver, which is represented by α_R (purple coverage). A wide FoV can cope with movements at the transmitter, but captures more noise.

Our toolbox, based on the above described model, is built upon Optometrika, a ray-tracing tool [18]. In essence, the toolbox divides the surface of the emitter, transmitter and receiver into small elements and calculates the fraction of rays that are able to reach the receiver. To assign the correct weight to each ray, Optometrika considers important optical parameters such as the angles of radiation, incidence and reflection. To analyze ambient light communication, the key inputs we need to provide to the toolbox are the radiation patterns of the emitter and the modulating surface.

---

[1]It is important to note that our model also captures the performance of retroreflectors because, from an optical perspective, the reflected radiation patterns are similar to those caused by mirrors
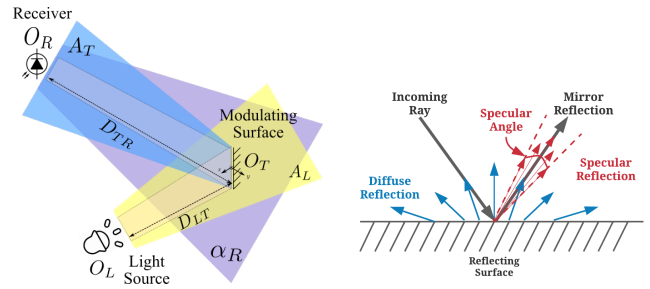
(a) A 2D representation of the optical system

(b) Different types of reflections based on the Phong model [19].

Figure 2: Optical system and different reflection types.

2.3 Insights & Guidelines

A passive link is, in essence, a triplet <emitter, transmitter, receiver> that finetunes the parameters of each element to optimize the performance. To analyze the complete design space, including the systems proposed in prior studies, we utilize a few abstractions for the emitters and transmitters, as presented in Tables 1 and 2.

Unless indicated otherwise, our analysis assumes that (i) there is no noise, which is similar to conducting experiments in the dark, (ii) the illuminance on the transmitter is fixed at 1800 lx, to provide a common baseline for all cases and *remove the trivial case where the performance is increased by increasing the illuminance*, and (iii) the area of the receiver is 1×1 cm^2. The selected area has no real impact on the analysis. The only assumption we make is that the transmitter's area is bigger than the receiver's, which is the case for most systems. Also, for our initial analysis, the receiver's FoV does not play a role because we assume a dark environment. In practice, the FoV plays a critical role and we will discuss it later on.

Regarding the modulating surface, we consider two main reflective patterns, as shown in Fig. 2b: *diffuse reflection*, caused by rough surfaces that reflect light in all directions, and *specular reflection*, caused by smooth surfaces. We further classify specular surfaces based on their specular angle. If the angle is zero, we call it mirror reflection.

2.3.1 Choosing the right emitter and transmitter

The design space of passive links can be divided into six main blocks based on the <emitter, transmitter> pair. Table 3 shows previous works categorized in this manner. Considering that direct sunlight provides tens of thousands of lx, overcast sunlight thousands of lx and light bulbs only hundreds of lx, a

Table 1: Emitters

Source	Type	Size of O_L	D_{LT}
L1	LED	5 cm × 5 cm	1 m
L2	LED	5 cm × 5 cm	4 m
L3	Diffuse Sunlight	N/A	N/A
L4	Direct Sunlight	N/A	N/A

Table 2: Transmitters

Modulating Surface	Type	Specular Angle	Size of O_T	Illuminance
T1	Diffuse	N/A	3 cm × 3 cm	1800 lx
T2	Specular	0.3°	3 cm × 3 cm	1800 lx
T3	Specular	1°	3 cm × 3 cm	1800 lx
T4	Specular	5°	3 cm × 3 cm	1800 lx

Table 3: A taxonomy of passive VLC systems

Light Source	Specular (includes retro-reflectors)	Diffuse
LED	RetroVLC [13] PassiveVLC [29] RetroTurbo [28] RetroI2V [25]	
Sunlight (Cloudy Day)		Tweeting with Sunlight (TwSL) [4]
Sunlight (Clear Day)	ChromaLux [7]	Luxlink [3]

designer may assume that for any given surface, sunlight will always perform better than light bulbs. Similarly, considering that specular (mirror) surfaces provide stronger reflections than diffuse surfaces, a designer may assume that for any type of ambient light, a specular reflector will always perform better. Neither assumption is correct. In fact, we show that a particular combination of sunlight and specular reflectors gives the worst performance.

Fig. 3 depicts the signal strength of various scenarios as a function of the transmitter-receiver distance (D_{TR}). We consider all six possible combinations of *emitters*: LED (L1 & L2), overcast day (L3), clear day (L4); and *transmitters*: diffuse (T1), specular (T2). Our results show four design regions, which are described next from worst to best. Our evaluation section validates many of these results empirically.

Region 1: cloudy day & specular surface (L3-T2 in Fig. 3a, gray area in Table 3). This region captures the scenario in Fig. 1d, where light arrives in a scattered manner and only an infinitesimal amount of the flux reaches the receiver. The signal strength of this setup is so weak and decays so fast, compared to the other scenarios, that it is not shown within the range of Fig. 3a to have a clearer view of the other regions.

Region 2: any light & diffuse surface (LX-T1, blue area). When a diffuse surface is used, it does not matter the radiation pattern of the light source, so long as the luminous flux at the transmitter's surface is the same. Note that all T1 curves overlap with each other in Fig. 3a. This occurs because ideal diffusers, such as paper or plaster, distribute the reflections of the impinging flux in all directions.

Region 3: LED & specular surface (L1/L2-T2, red area). This is the second best region, and coincidentally, the main focus of prior work using retro-reflectors. Artificial lights, however, offer a wide range of radiation patterns, resulting in widely different performance. To illustrate this point we use Fig. 3b, where two emitters are placed at 1 m and 4 m (L1 & L2). *Both emitters attain the same illuminance at the receiver* (1800 lx, a white light illuminance of 1800 lx over an $1 m^2$ surface is approximately equivalent to the power of a 25 W LED), but L2, which is *further away*, provides a stronger signal strength, which is counter-intuitive. This

occurs because the further away the light source is, the more it behaves as a distant point source, leading to more directional beams impinging on the transmitter, and hence, less flux lost towards the receiver, c.f. Fig. 1c. In practice, L1 could be seen as a light bulb and L2 as a flashlight, which explains why studies using a flashlight attain better results [25, 28].

Region 4: clear day & specular surface (L4-T2, green area). This is the best operation region. Note that the signal strength hardly decays in Fig. 3a. This occurs because the high directionality of clear sunlight maintains the luminous flux over long distances, which is why heliographs (mirrors) used in the 1800's reached ranges beyond 100 km. This same property can increase the data rate of ambient light links. In practice, air attenuates the signal strength (similar to what happens with lasers), but the benefits of directionality remain strong.

2.3.2 Choosing the right specular surface

The above analysis highlights the importance of maintaining directionality throughout the optical link. However, given that there are no perfect mirror-reflectors, how critical is the specular angle? A wide specular angle can be the result of imperfections on the surface. For example, many studies use retro-reflectors, but the quality of retro-reflectors can vary. Fig. 3c shows the signal strength of surfaces with different specular angles, from narrow (T2, 0.3°) to wide (T4, 5.0°), considering an LED (L1) and direct sunlight (L3). When an LED is used (blue lines), the misaligned radiation pattern of the LED is more relevant than the specular angle, therefore, there is not much difference among the various surfaces. However, for a directional source (red lines), a large specular angle (e.g. 5° for T4) can lead to a significant decrease in the signal strength. Thus, *the more directional the rays, the more critical is the use of high-quality specular surfaces.*

2.3.3 Choosing the right receiver

Passive-VLC systems use cameras and photodiodes as receivers. Cameras are widely available in smartphones, but they are power hungry and slow, allowing only a few hundred frames per second. Photodiodes (PDs), on the other hand, are inexpensive, low-power and have a high bandwidth. Thus,
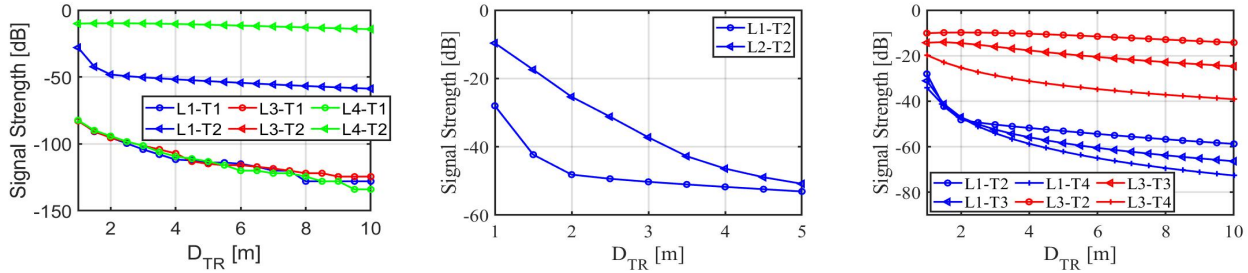
(a) Signal strength for different light source and surface combinations

(b) Signal strength for LEDs at different distances D_{LT}.

(c) Signal strength for different specular angles.

Figure 3: Different simulation setups.

PDs are the preferred choice for high data rate links. A key element in the PD's design is its FoV. The FoV will not only capture the intended signal but the surrounding noise as well (purple coverage in Fig. 2a). In practice, to maximize the SNR, the receiver's FoV should cover only the modulating surface, but that is difficult to attain. PDs with varying FoV have been used in the literature, ranging from $1°$ to close to $90°$ [3, 26]. Many studies using the wide FoV, however, were conducted at night with no interfering ambient light, which is similar to having a nearly perfect FoV of $0°$. Given that our system is aimed at working with surrounding ambient light (noise), we borrow the design from [3], which uses a lens at the receiver to reduce the FoV, and thus, limit the noise level.

Overall, our analysis uncovers two key design guidelines. First, for the emitter-transmitter link. Direct sunlight, flashlights and light bulbs –in that order– are preferred due to their directionality. Diffuse (cloudy) daylight is the least ideal condition in spite of being the second most powerful source (after direct sunlight). Second, for the transmitter-receiver link. The more directional the light source is, the more critical is to use mirror-like reflectors. The only case where diffuse surfaces are preferred is when the impinging light is diffuse as well.

3 Transmitter Design

3.1 LC limitations

Most passive-VLC systems using either transmissive [3, 30] or reflective (backscattering) principles [13, 29] rely on liquid crystal shutters (LCs) as the modulating surface. Unlike liquid crystal displays (LCDs), LCs do not have embedded light sources. LCs are readily available, economical, and power efficient, but they suffer from two intrinsic limitations.

3.1.1 Limitation 1: High signal attenuation

LCs only allow a single polarization direction to pass through. All other directions are either fully or partially attenuated. Ambient light, however, is not polarized. This implies that only half of the power can pass through a linear polarizer. On the other hand, DMDs have microscopic mirrors with a high reflection coefficient and are polarization insensitive. For example, the DLP2000 module from Texas Instruments has an efficiency of 97% [9]. Thus, considering the same modulating area and incoming illuminance, DMDs radiate almost 100%

more light than LCs, which can be exploited to increase the range or the data rate of passive links.

3.1.2 Limitation 2: Limited bandwidth

The rise and fall times of commercial LCs take a few ms, as shown in Fig. 4d. These times limit the bandwidth to be under 1 kHz. Furthermore, LCs combine two different operation principles, an electrical signal for the rise time and mechanical inertia for the fall time. This asymmetric operation makes the fall time much slower and it is usually the main bottleneck to increase the bandwidth. Active research has been carried out to squeeze as much data rate as possible from that limited bandwidth, but community efforts are still restricted to around 1 kbps for single-cell designs [3,7,13,29] and 8 kbps for more sophisticated multi-cell designs [25, 28]. DMDs, on the other hand, use the same (fast) operating principle for the rise and fall times. We exploit this fast switching speed to increase the data rate of passive links by an order of magnitude or more.

3.2 DMD basics

A DMD is an optical micro-electro-mechanical system (MEMS) that contains between a few hundred thousand and several millions of highly reflective microscopic mirrors of less than 10 microns each. A DMD can be controlled by electrical pulses, which flip each mirror to one of two fixed directions, for example, $+12°$ and $-12°$. DMDs usually come integrated within a sophisticated projector system called Digital Light Processing (DLP). Besides the DMD, the DLP has a lamp, a light absorber and a projection lens, as shown in Fig. 4a. A micro-mirror is *on* if its angle is tilted towards the projection lens, and *off* if the angle is tilted towards the light absorber. All these optical and electrical components are tightly synchronized by the DLP controller.

There are multiple types of DLPs, as shown in Table 4. All these DLPs tackle *Limitation-1* because DMDs have a high reflective coefficient by design, but exploiting the DMDs' potential for higher bandwidth is harder to attain (*Limitation-2*). On one hand, there are inexpensive units, such as the DLP2000 ($\sim$ €100), but their screen refresh rate is too slow. The refresh rate can be seen as the equivalent of the rise (or fall) time in an LC. At 120 Hz, the DLP2000 is even

(a) States: ON/OFF (right/left pixel). Reprinted from [12].

(b) Maximum data rate of out-of-the-box DMD

(c) DMD rise/fall time with custom controller
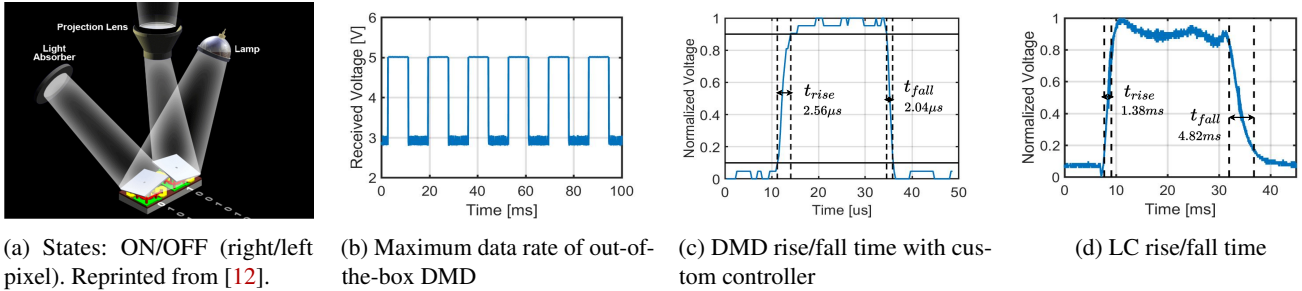
(d) LC rise/fall time

Figure 4: DMD Pixel states and DMD and LC timing characteristics.

slower than the LC shown in Fig. 4d, which provides 320 Hz ($\frac{1000 \times 2}{1.38 + 4.82}$). On the other hand, there are units providing refresh rates above 20 kHz, but with prices beyond €4K, they are prohibitively expensive compared to LC-based systems, which cost a few tens of Euros. A single DMD device (instead of an integrated unit) has comparable cost (€26) to a LC.

The inability to exploit DMDs is an important barrier in passive-VLC. While there are multiple studies utilizing LCs, there are only a few utilizing DMDs. One of those studies uses the same DMD we use, the DLP2000, but attains only a few bits per second because they only use the default refresh rate (120 Hz) and utilize a smartphone camera as a receiver, which is inherently slow [2]. The other studies utilize the more sophisticated DLP4500 (€1100) [10, 11], which provides a maximum refresh rate of 4.2 kHz. Those studies, however, do not exploit that refresh rate for digital communication, but to generate analog signals of just a few tens of Hz (sine, square, triangle, saw-tooth) for localization and audio transmissions. We design a controller for the inexpensive DMD inside the DLP2000 (€26) and increase its refresh rate to 220 kHz, almost a factor of ten faster than the most expensive DLP (DLP9500, €4400). Next, we describe the main limitation of the DLP2000 for ambient light communication, and subsequently, the design of the PhotoLink controller.

3.3 Limitations of inexpensive DMDs.

The DMD from the DLP2000 is the most readily available and economical product, but it is designed for display applications. Hence, for ambient light communication, logical 1s and 0s can only be conveyed as a series of white and black images in a video, which leads to the slow update rate shown in Fig. 4b. In a video application, the pixel's color is obtained by (i) multiplexing RGB beams and (ii) changing the duty cycle of the mirror for each color beam. DMDs provide incredible images, with up to 16.7 million colors, thanks to the fine-grained duty cycle provided by the micro-mirrors. *The micro-mirrors can be flipped at very high speeds between their on/off status*, enabling short operational periods τ, with $\tau \ll T$. These short periods allow a large number of (primary color) combinations. The operation of DMDs, however, is designed for the human eye, which has a slow response. As long as the $3T$ period takes less than 8.3 ms (120 Hz), people will only see high quality videos. Photodiodes, on the other hand, have MHz bandwidth and do not need to capture colors. For
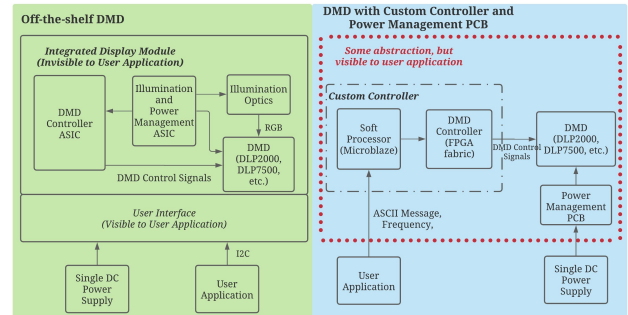

Figure 5: The block diagrams of an off-the-shelf DMD (green, left), and our custom PhotoLink controller (blue, right)

PhotoLink, we need control of τ, not T. Thus, our goal is to remove the controller in the original system and design a new one that gets us as close as possible to the bare fast switching speed of the micro-mirror.

3.4 PhotoLink controller

There are two main obstacles preventing the use of inexpensive DMDs for ambient light communication: no suitable *hardware abstractions* or *operational modes*. Next, we describe each obstacle and the solutions we provide.

3.4.1 Hardware abstraction

Most commercial DLPs do not expose control and power signals to user applications, as illustrated in Fig. 5. There are two ASIC components preventing direct access to these signals: the controller and power management. The *controller* implements the logic to set each micro-mirror and an I2C interface. The interface is the only means to communicate with user applications and hides all control signals. It is therefore impossible to extend beyond the supported frame rate by the controller (120 Hz for the DLP2000). The *power management* controls the DMD power and the integrated RGB light source, which is not needed for ambient light communication.

To increase the refresh rate of the DMD, we remove all hardware components from the original DLP design and use only the DMD. As shown in Fig. 5 (blue side), our main components are: (i) the power management unit, which provides the necessary voltage supplies for different DMD operations without requiring a light source; (ii) an FPGA, which supplies

Table 4: Commercial DMD Module

Name	Clock Rate	Data Bus	Screen Refresh Rate	# of Pixels	Module (DLP) Price	DMD Price	# of pins
DLP2000	60-80 MHz	12(bits)x1	120 Hz	640x360	€109.01	€26.14	42
DLP4500	80-120 MHz	24(bits)x1	4.2 KHz	912x1140	€1106.49	€144.69	80
DLP7000	200-400 MHz	16(bits)x2	32.5 kHz	1024x768	€4144.09	€866.96	203
DLP9500	200-400 MHz	16(bits)x4	23.1 kHz	1920x1080	€4403.30	€2693.38	355

the data and logic for updating the DMD; and (iii) the Microblaze module (soft-processor), which runs on the FPGA and provides a user interface but without hiding the control logic. This interface is used to configure the packet format and the transmitting frequency (explained in section 4).

3.4.2 Operational modes.

Creating a new hardware abstraction is necessary but insufficient to use the DLP2000 for ambient light communication. The next step is to apply the appropriate operational mode to switch the mirrors as fast as possible. The manufacturer does not disclose all the required information to tackle this step, so we base our design on two references: the data sheet of the DMD [9] and a basic description of micro-mirrors [12].

The switching of the mirrors involves two steps: the *memory state* and *micro-mirror state*. In the memory state, the value of each mirror is set (on/off), but the mirror does not tilt. In the micro-mirror state, an actuation pulse tilts the mirrors to their new value. These states define two operational modes.

Individual pixel mode. In this mode, every pixel acts as an individual binary reflector. This allows the DMD to be configured as a fine-grained video projector. The DLP2000 has more than 230 thousand pixels, whose memory has to be written sequentially. As a result, the memory state takes a few hundred μs before any actuation (transmission) can be performed.

Global mode. Considering that the bulk of the delay is in the *memory state*, it would be ideal to by-pass it. In ambient light communication, a fine-grained control of the DMD is not necessary, as photodiodes are used as receivers[2] It is sufficient to update all pixels at once and use the DMD as a single-pixel device, which we dub the global mode. In this mode, we do not write the memory of each pixel, but instead write a global '0' or '1' to all pixels. Attaining this operation requires a careful coordination of various signals[3], but the bandwidth increases dramatically compared to the original DLP design, as shown in Fig. 4c: 60 Hz vs 217.4 kHz, a factor of 3600+[4]. Compared to the LC, the global mode reduces the rise time by a factor of 540 (2.56 μs vs. 1.38 ms) and the fall time by a factor of 2360 (2.04 μs vs. 4.82 ms), which translates to almost a 1350 increase in bandwidth.

---

[2]To take advantage of the individual pixel model, a camera has to be used as a receiver, which is slow (hundreds of frames per second) and requires the use of large screens as transmitters to be efficient.

[3]The hardware and firmware of our controller will be made open source.

[4]The refresh rate of the DLP2000 is 120 Hz, which considers only the time taken by the rise or fall time, the bandwidth considers both times.

3.4.3 Summary of contributions.

Our novel controller allows inexpensive DMDs to be decoupled from their integrated video-projection system. We design a global mode to take full advantage of the fast switching times of micro-mirrors. Compared to LCs, our approach increases the transmitter bandwidth by more than three orders of magnitude. Our controller also achieves a higher refresh rate, even when compared to the high-end DLPs shown in Table 4. Since all DMDs manufactured by TI follow the same operating principles [12], our controller's design would also apply to those DLPs, which could allow them to increase their refresh rates to attain even a better performance than the one obtained with the low-end DLP2000.

4 Optical Link

4.1 Modulation

The majority of modulation schemes fall within two categories: amplitude-based [13, 29] and frequency-based [3]. Amplitude-based methods work well in dark scenarios but are prone to errors when external light sources are present. Frequency-based modulation, on the other hand, has the inherent property of being more resilient to external noise. However, prior LC studies using frequency-based methods had difficulties creating stable periodic signals because the rise and fall times of LCs are asymmetric [3]. DMDs have symmetric times, which allows the generation of stable periodic signals.

To increase the data rate, we use M-ary FSK (MFSK) with two bits per symbol. This high frequency band of PhotoLink (217.4 kHz) allows us to define different modulation parameters and data rates, as shown in Table 6. For example, for a data rate of 30 kbps, we set the four modulating frequencies to 15 kHz, 30 kHz, 45 kHz and 60 kHz. The different modulation parameters permit a thorough evaluation of PhotoLink under different ranges and with different receivers, as discussed in the next section. To avoid abrupt transitions between two frequency signals, the transition between the MFSK frequencies only occurs after a full oscillation period, as depicted in Fig. 6. Considering that the only prior work using MFSK for passive-VLC is [3], we use it as a baseline for comparison. We implement a similar data link layer (shown in Table 5) and receiver design (shown in Fig. 7b and described in Sec. 5). Our packet starts with a SYN symbol (00010101) that uses only the lower transmitting frequencies (00 & 01). These low frequencies have the highest amplitude, and hence, it is easier for the receiver to discover the signal and synchronize to the phase of the transmitter. The ASCII payload is preceded by a STX (Start of Text, 00000010) and followed by ETX (End

Table 5: The structure of the data link layer.

00010101	00000010	ASCII Byte Array	00000011	00010111	00010101
SYN	STX	ASCII Text Message	ETX	ETB	SYN

Table 6: Parameters for different bit rates.

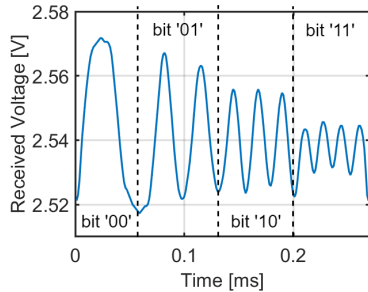| Bit rate	Symbol	Frequency	# of cycle
24 kbps/30 kbps/ 40 kbps/60 kbps/ 80 kbps/100 kbps	00	12/15/20/30/40/50 kHz	1
	01	24/30/40/60/80/100 kHz	2
	10	36/45/60/90/120/150 kHz	3
	11	48/60/80/120/160/200 kHz	4

Figure 6: The received signal for different symbols for 100 kbps. Each symbol carries two bits.

of Text, 00000011) and ETB (End of Transmission Block, 00010111).

4.2 Demodulation

The receiver knows the transmitting frequencies and takes the following steps to demodulate the signal.

Preamble detection: A sliding window, equivalent to one symbol, applies a Fourier transform (FFT) to the received signal and decodes the symbol. Every time a byte (four symbols) is decoded, the byte is compared to SYN.

Data demodulation: After a SYN byte is identified, the receiver decodes the incoming message using the same FFT process. If an ETX is received, the packet transmission ends.

Phase correction: If a received two-bit symbol is '00', during the preamble detection or data demodulation, the receiver leverages the presence of this high-amplitude symbol to synchronize to the phase of the transmitter and adjust to any frequency shift that could have been induced by the channel.

5 Evaluation

Our transmitter runs the methods described in Sec. 3 using a custom FPGA controller board and a custom PCB with power management circuits for the DMD. Next, we evaluate our simulation toolbox and controller under various aspects.

5.1 Receiver Design & Data Rate

The design of a low-power optical receiver needs to balance a trade-off between gain and bandwidth. If we optimize for sensitivity (high-gain), small changes in light intensity can be detected, which is advantageous for long-distance communication; but the response is slow (low-bandwidth), which limits the ability to decode high frequency carriers. The opposite trade-off holds for a high-bandwidth receiver. A low-

(a) Transmitter setup   (b) Receiver setup

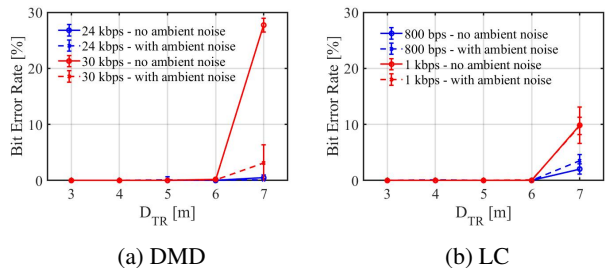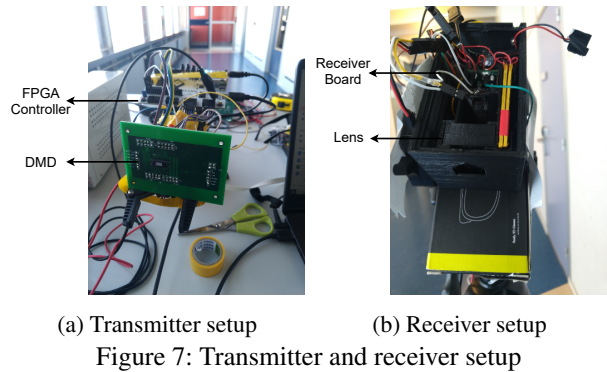Figure 7: Transmitter and receiver setup

(a) DMD   (b) LC

Figure 8: Bit error rate of DMD and LC with artificial light

bandwidth receiver is not a concern when LCs are used as transmitters, as the bandwidth of the LC is low, but it can severely restrict the performance of DMDs. In this subsection, we compare the performance of PhotoLink with LCs used in state-of-the-art studies. we quantify the performance of PhotoLink with two receivers, one optimized for LC operation and the other for DMD. LCs can be used in different ways depending on the type of application: as part of a reflective tag, where either a diffusive or retro-reflective material is placed behind the LC to reflect light, or as part of a transmissive tag, where the LC is used solely as an optical shutter without additional reflective surfaces. To ensure a fair comparison between DMDs and LCs, in the following evaluation, we carry out experiments with both optical devices, but without adding any additional surfaces.

Experiment 1: Receiver optimized for LCs. PhotoLink increases the data rate by a factor of 30.

In this experiment, we use a receiver similar to the one used in [3], consisting of a convex lens with a diameter of 2.5 cm and a TEPT4400 photosensor placed at the focal distance of the lens. The TEPT4400 is a high-gain low-bandwidth photoresistor well-suited for long-range communication with LCs. Using the same illumination environment, we test this receiver using a DMD and an LC as transmitters. The LC and the DMD have the same physical setup, surface area, modulation and demodulation schemes.

Table 7: Rise and fall time for different sensors and resistors

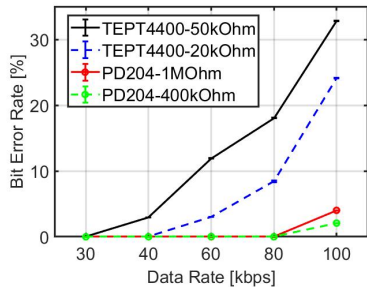| Photoreceiver	Feedback resistor	rise time	fall time
TEPT4400	69/50/20 kΩ	100/64/24 μs	140/105/48 μs
PD204-6C	1000/400/100 kΩ	6.4/3.5/2.5 μs	6.2/3.2/2.1 μs

Figure 9: Bit error rate with different sensors and resistors.

We evaluate the DMD and LC in two scenarios. First, we use a bike flashlight (Simson USB Headlight "Future") to illuminate the transmitting surface in a dark room, such that repeatable experimental results can be obtained. The flashlight is placed 1 m away from the transmitter, and the illuminance at the transmitter is 1800 lx. Then, we use the same setup but turn on the indoor lights located on the ceiling and allow natural ambient light to enter the room (in addition to the flashlight). These additional light rays are not aligned with the receiver and act as ambient noise. The illuminance of the ambient noise (excluding the flashlight) is around 700 lx at the transmitter.

In each experiment, a "Hello world!" packet is sent 100 times. Each experiment is repeated 30 times, and the mean and standard variation of the bit error rates are shown in Fig. 8. With the DMD, we obtain an average BER of less than 1% at 7 m for a data rate of 24 kbps and 6 m for a data rate of 30 kbps. With the LC, we obtain an average BER of less than 1% at 6 m for a data rate of 800 bps and 1 kbps. The data rates achieved with the LC are in line with what has been reported for single-pixel systems [3, 7, 13, 29]. Overall, under the same illumination and modulation conditions, DMDs achieve a data rate of more than 30 times that of LCs.

Experiment 2: Receiver optimized for DMDs. PhotoLink increases the data rate by a factor of 80.

Considering that the maximum data rate achieved by the SoA is 8 kbps [28], a 30 kbps link is a significant improvement. However, using a receiver optimized for LCs does not exploit fully the capabilities of DMDs. Note from Table 6 that the maximum frequency used for a 30 kbps data rate is 60 kHz, but as stated in section 3, the global mode can reach frequencies above 200 kHz. The limitation of low-bandwidth sensors is that they cannot capture fast transitions: even though the *transmitted* signal has rise and fall times below 3 μs (Fig.1c), the *received* signal delivers rise and fall times above 100 μs.

At the core of this phenomenon are two parameters, the parasitic capacitance C_P, which is inherent to the sensor and cannot be modified; and the feedback resistor R_F, which can be modified. A large R_F and C_P improve the receiver's SNR

(high-gain), but reduces the bandwidth. We analyze the effect of the feedback resistor on two photosensors: the TEPT4400 (high C_P, low-bandwidth) and the PD204-6C (low C_P, high-bandwidth). Table 7 shows the ability of each receiver-resistor pair to measure the fast DMD transitions for the rise and fall times. The first pair is the configuration used for LCs in [3], and thus, we use it as our baseline. We can see that the PD204 has a bandwidth that is big enough to capture transitions in the few microseconds range.

To showcase the importance of designing an optimal receiver for DMDs, we select four pairs from Table 7, and repeat the same experiment and setup described in Sec. 5.1 but for a fixed distance d_{tr}=2 m. The results are presented in Fig. 9. We know from *Experiment 1* that the TEPT4400 with a 69 kΩ resistor can attain 30 kbps (baseline). A 50 kΩ resistor is not low enough to increase the bandwidth significantly, but a resistor of 20 kΩ can increase the data rate to 40 kbps. The lower capacitance of the PD204, however, increases the bandwidth to a value that is high enough to double the data rate, reaching 80 kbps. Note that the improvement in data rate comes at the cost of reducing the range (lower gain). For the TEPT4400, the range is reduced from 6 m (30 kbps) to 2 m (40 kbps). For the PD204 with 100 kΩ (last pair in Table 7), the data rate reaches 100 kbps but at ranges shorter than 2 m, and thus, is not presented in Fig. 9. The limited range, however, is not a fundamental problem because it can be increased by adding more amplifier stages at the receiver (our receiver has a single stage) or by using focusing lenses at the transmitter. In the case of the LCs, the bandwidth of any photodetector is much higher than the the bandwidth of the LCs, however, that is not the case for DMDs. We expect that an even higher data rate can be achieved if a photodetector with a high gain bandwidth is used together with multiple stages of signal amplification. The data rate, on the other hand, has been a fundamental limitation for passive-VLC and PhotoLink provides a ten-fold improvement over the most sophisticated LC-system in the SoA. Regarding the cost, DMD-based and LC-based systems can make use of the same photo-receivers, a DMD (€ 28.62) costs € 22 more than an LC (€ 6.56). We use an Artix-7 FPGA, which cost € 50, but a less expensive controller can be used as well. A microcontroller that costs € 13.6 was used in Luxlink [22].

5.2 Analyzing the Luminous Flux

Our work has two main contributions, the controller evaluated in the prior subsection and the toolbox presented in section 2. The main insight of our toolbox is the importance of maintaining the luminous flux throughout the optical link. To capture this phenomena, we consider two scenarios.

Scenario 1: Normalized flux (indoor setup). In this scenario, we use the baseline receiver (TEPT4400 with a 69 kΩ resistor) and transmit a fixed carrier frequency. The frequency is empirically chosen to be 30 kHz because this signal can be clearly detected at 4 m without saturating the receiver at 1 m. To calculate the amount of luminous flux maintained

in the optical link, the signal intensity measured at 4 m is normalized with respect to the intensity measured at 1 m for *the same* light source. This normalization process and careful setup quantify the impact of the radiation pattern of each light source independent of its emitted power.

Under this setup, we evaluate four different light sources *indoors*, as shown in Table 8, and simulate the same illumination conditions with our toolbox. In the test setups, the direct and diffuse sunlight arrive at the DMD through a large glass window. To obtain realistic simulation results, we apply the parameters in Table 9, which correspond to the actual physical properties of PhotoLink. The normalization method is also applied to the simulations[5], and the results are shown in Fig. 10. The plots show a strong agreement between the experimental and simulated flux under all illumination conditions. With diffuse sunlight, we are not able to detect a signal even at 1 m, despite measuring a 2000 lx illuminance on the surface of the DMD. This aligns with our analysis in Sec. 2, which states that diffuse light has the lowest performance with reflective surfaces. The results also show that direct sunlight performs best at retaining the luminous flux (losing 30% at 4 m), followed by artificial lights (losing more than 80%). And with artificial lights, more luminous flux is retained at the receiver when the light is placed further away from the transmitter (setup 2). All these results are in agreement with the insights provided by our model in Sec. 2.

Scenario 2: Absolute flux (outdoor setup). In this scenario, we do not perform a normalization process, instead, we transmit 100 packets of "Hello world!" at 30 kbps and present the received voltage and BER. We evaluate the two best light sources identified by our toolbox, flashlight and direct sunlight. The evaluation with direct sunlight is done *outdoors* during a clear day with good sunlight (several thousand lux), and then, moving the setup indoors and placing a flashlight in a dark room.

With sunlight, a BER of $0.9x10^{-3}$ is achieved at 1 m and a BER of $0.8x10^{-3}$ is achieved at 2 m. The errors can be attributed to the fact that a link in the outdoor environment is subjected to occasional disturbance. With flashlight, the BER is 0 at 1 m, however, at 4 m, the BER increases to $19.4x10^{-3}$. In Fig. 11, we present a direct comparison of the flux reaching the receiver with the flashlight and sunlight using the SYN symbols in the packet. At 1 m, the flux reaching the sensor with the flashlight is slightly lower than that with sunlight (around 0.18 V vs. 0.2 V), which shows that the flashlight and sunlight result in similar voltage range. However, at 4 m, the luminous flux reduces by 60% with flashlight, due to a less directional pattern, while direct sunlight loses only 10%[6]. This result highlights the importance of expanding passive-

---

[5]Since photodiodes have a quasi-linear response to light intensity, we assume a linear correlation between the obtained signal strength in the toolbox and the voltage obtained in our experiment.

[6]Note that the flashlight loss is higher than the loss predicted in Fig. 10 for 1 m because we place the light closer to the DMD, 30 cm instead of 1 m

Table 8: Measuring the power drop-off with respect to distance

Setup	Light Source	D_{LM}	D_{TR}	Measured Normalized Signal	Simulated Normalized Signal
1	Direct Sunlight	N/A		0.70	0.73
2	Flashlight	4 m	1 m and 4 m	0.17	0.20
3	Flashlight	1 m		0.04	0.06
4	Diffuse Sunlight	N/A		N/A	N/A

Table 9: Key parameters used in simulator

Light Source	Dimension	2.7 m x 2.7 m
	Half Angle	30°
Modulating Surface	Dimension	4.8 mm x 2.7 mm
	Light-absorbing area	8 mm by 8 mm
	Spreading Angle	0.3°
Receiver	Lens Dimension	2.5 cm
	Tangent Sphere Radius	(4 cm, -5 cm)
	Lens Material	bk7
	FoV	1°
	Photodiode Diameter	3 mm

VLC studies towards the exploitation of natural light.

5.3 Issues with DMDs

DMDs have not been designed for ambient light communication, and hence, present some limitations. We now discuss what we consider the main shortcomings of this MEMS technology for passive-vlc.

Issue 1: Directionality. DMDs operate with two fixed angles, which raises up the issue of directionality. If the light source changes its location, the impinging light rays will no longer be aligned with the predefined angles at the DMD, breaking the link. This issue can be overcome with light concentrators. As a proof of concept, we build a simple concentrator with two optical components, as show in Fig. 12a. The first component is a Compound Parabolic Concentrator (CPC). The CPC is a special parabolic lens that collects light from different angles and concentrates it on a small output area. We use a CPC with an input and output circular area of 14 mm and 4 mm diameter respectively, and a concentration factor of 10. The second component is a ball lens of 8 mm diameter, which is used as a coupler and collimator, to further focus the collected light. We manufacture a 3D-case to align the CPC and the ball lens, and aim its output to the DMD.

Fig. 12b presents the results obtained with and without the light concentrator. A flashlight is positioned at different incidence angles and the signal strength is measured at the receiver. Without the concentrator, the signal strength decays below 0.9 with deviations around +/- 1 degree. With the concentrator, the signal remains above 0.9 for angles around +/- 10 degrees. This is a simple implementation, more sophisticated designs can increase the FoV to any desired degree. Thus, while an ideal DMD design for passive-VLC could consider flexible angles, it is not a strict requirement.

Issue 2: Power consumption. Perhaps the most limiting factor of current DMD designs is the relationship between its small area and relatively high power consumption. The
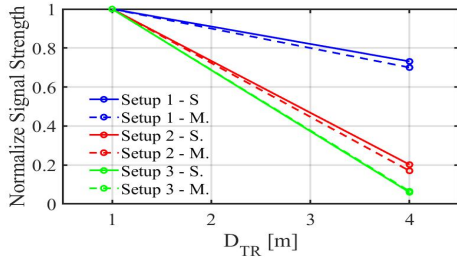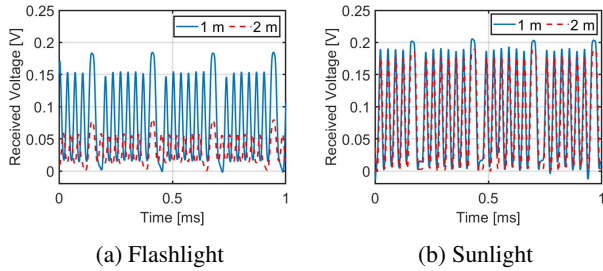
Figure 10: Simulated and measured voltage dropoff.

(a) Flashlight   (b) Sunlight

Figure 11: Signal strength


(a) Design   (b) Evaluation

Figure 12: CPC

performance of passive-VLC depends on the area of the transmitting surface. For example, a standard light bulb consumes 1 watt to emit 90 lumen,But with an area of 13 mm^2, the DLP2000 would emit only between 0.1 and 0.5 lumen.

Regarding the power consumption, current DMD designs have two levels of overhead. The first level is related to the *memory state*, which is not required for PhotoLink and consumes 57 mW in the DLP2000. The second level is the actuation of the micromirrors and consumes 45.5 mW. We are, thus, left with a surface that emits between 0.1 and 0.5 lumen (depending on daylight conditions), while consuming 45 mW. Considering that LCs consume less than 1 mW, and that low-power LEDs consume less than 100 mW, it is central to consider power consumption in the comparison with LCs and LEDs. To perform that analysis, let us consider a low-power LED that has been used in prior VLC studies [8], the VLMB1500, which consumes 75 mW and emits 0.2 lumen. We perform a theoretical comparison between LCs, DMDs and LEDs based on the Shannon-Hartley theorem $C = B \log_2(1 + SNR)$. The analysis assumes a luminous flux of 0.2 lumen for the DMD.

First, let us consider LCs, which have areas that are two orders of magnitude bigger than DMDs, and hence, receive two orders of magnitude more lumen. Assuming that the LC receives 20.2 lumen on its incoming area (20 from the light source and 0.2 from the 'extra' LED), the outgoing flux would be 10.1 lumen because LCs cut the power in half (Limitation-1 in section 3). Hence, the SNR of an LC-system would increase by a factor of 50 (10.1/0.2), but the SNR only contributes logarithmically to the capacity. Overall, the extra SNR would contribute with a factor of 6, compared to the factor of 1350 contributed by the BW of the DMD, making the DMD still two orders of magnitude more competitive.
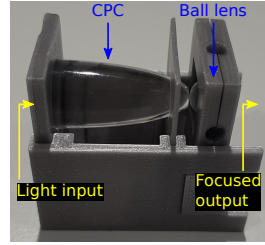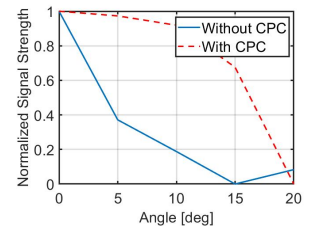
To consider the option of using the LED with active-VLC, we measure its rise and fall times, which are 3.5 µs and 1.6 µs: a period of 5.1 µs compared to the period of 4.6 µs for DMDs. Recalling that the LED and DMD emit a similar lumen, the DMD is only slightly more competitive. This result, however, should consider that current DMDs are not designed for ambient light communication. The mirrors of the DLP have a size of microns and use *electrostatic* actuation, larger area mirrors (bigger than 2 mm) "benefit from *electromagnetic* actuation proportional to the mirror area" [17], leading to bigger surfaces with lower power consumption.

Thus far, the passive-VLC community has faced a major obstacle, even with big LC surfaces, no system can provide data rates above 10 kbps. PhotoLink shows that current (suboptimal) DMDs can provide 100 kbps. Synergies with MEMS researchers could enable the design of bigger modulating surfaces to create wireless networks operating solely with natural light and with low power budgets.

6 Related Work

Passive VLC systems using LCs. There have been several studies on passive VLC systems, which are summarized in Table. 10. To date, LCs have been widely used as an optical transmitter in SoA passive VLC systems. There are two categories: one uses LCs in combination with retro-reflectors, where the light source and the receiver are co-located; the other adopts only the LC as a transmitter, where the light source and the receiver can be placed at different locations, opening up the possibility to take advantage of natural light.

The studies in the former category typically have a constrained data rate and range. The earlier studies [13, 29], achieve a data rate of 0.5 kbps and 1 kbps with ranges up to a few meters. More recently, RetroI2V [25] achieves a range of 80 m. However, it uses a powerful 30 W light to achieve a data rate around 1 kbps. RetroTurbo [28] has a surface area of 66 cm^2 and uses an advanced modulation scheme to overcome the slow time response of LCs. RetroTurbo achieves a data rate of 8 kbps with a moderate light source (4W flashlight) up to 7.5 m [25]. However, retro-reflectors cannot be used with ambient light, as the light source and the receiver have to be co-located. On the other hand, the studies in the latter category take advantage of the strong illumination from sunlight and are able to achieve a long range without a dedicated illuminator, such as in the case of Luxlink [3] and Chromalux [7]. Luxlink is able to reach a range of 65 m with sunlight, but the

Table 10: Comparison of PhotoLink with the most relevant systems in the state of the art.

Name	O_L	O_L Power or Illuminance	D_{LT}	O_T	Surface Type	O_R	FoV	Data Rate	Range
RetroVLC [13]	LED	12 W	Variable[1]	LC+RR[2]	Specular	Photodiode	50°	0.5 kbps[2]	2.4 m
PassiveVLC [29]	Flashlight	3 W	Variable	LC+RR	Specular	PD	4°	1 kbps	1 m
RetroTurbo [28]	Flashlight	4 W	Variable	LC+RR	Specular	PD	20°	8(4) kbps	7.5(10.5) m
RetroI2V [25]	Flashlight	30 W	Variable	LC+RR	Specular	PD	30°	125(1000) bps	101(80) m
Chromalux [7]	Sunlight(Direct) / Flashlight	3-6 klx / 400-700 lx	N/A / N/S	LC and Metal Sheet	Specular	Color Sensor	Variable	1 kbps	50 m / 10 m
Luxlink [3]	Sunlight(Direct) / LED	10-26 klx / 2 klx	N/A / N/S[3]	LC and Diffuser	Diffuse	PD	1°	80 bps / 1 kbps	65 m / 3 m
TwSL [4]	Sunlight(Diffuse)	3 klx	N/A	Paper	Diffuse	PD	N/S	127 bps	4 m
[10]	LED	15 W	c̃ms	DMD	Specular	PD	N/S	4.2 kbps	170 cm
[11]	LED	15 W	c̃ms	DMD	Specular	PD	N/S	9 bps	2.5 m
[2]	Sunlight(Direct)	330 lux	N/A	DMD	Specular	Camera	N/S	1 bps	60 cm
PhotoLink	Flashlight	1800 lx	1 m	DMD	Specular	PD	1°	30(80) kbps	6(2) m

[1] For work involving retro-reflectors as a transmitter, $D_{LT} = D_{TR}$.
[2] RR stands for Retro-reflectors.
[3] For work involving retro-reflectors, uplink data rate is quoted.
[4] N/S stands for 'not specified'.

data rate is limited to 80 bps. It also demonstrates that with an LED, a data rate of 1 kbps can be achieved up to 3 m. Chromalux [7] takes advantage of the transient state in LCs, and is able to achieve a range of 50 m with a data rate of 1 kbps with sunlight, and up to 10 m with a flashlight. While LCs are energy efficient, they suffer from a high attenuation loss due to the use of polarizers, and a limited bandwidth because of its slow rise and fall times. On the other hand, a higher data rate can be achieved with DMDs, but using more power. And in addition to demonstrating a novel system, we provide an analytical framework to understand the performance of different studies.

Applications of DMDs. Like LCs, the main application of DMDs is video projection, and thanks to their competitive advantages (high reflective efficiency and switching times) they dominate the market. But DMDs are also used in other applications: microscopy, holography, data storage, and also as spatial modulators with lasers [6]. The use of DMDs for ambient light modulation, however, is restricted to a handful of studies involving localization [10] and communication [2, 11]. And all these studies suffer from a limited data rate (1 bps, 9 bps and 4 kbps), as well as a limited communication range (60 cm, 2.5 m and 170 cm). These systems use the off-the-shelf DMD controllers with their default refresh rates, which fail to take advantage of the fast switching times of the DMDs.

Channel modelling for VLC systems. There have been an array of studies on channel modelling techniques for indoor active VLC systems [21], several of which are ray-tracing based [15, 16]. The focus of those studies is to achieve an accurate impulse response considering the dynamics of the VLC system and its indoor environment. They remain a theoretical exercise in most cases, as an accurate description of the indoor space is difficult to obtain. This differs from our work, as our study focuses on the interactions between different types of surfaces and ambient light.

Ambient RF backscatter systems. In RF backscatter, passive devices can communicate with each other utilizing surrounding RF sources. The first study exploited TV tower signals and showed a data rate of 1 kbps at distances of 2.5 feet outdoors and 1.5 feet indoors [14]. Subsequent studies have shown that WiFi, BLE and LoRa signals can also be backscattered, attaining even higher data rates and/or ranges [1, 24]. RF backscattering is an exciting area but requires *man-made* signal (radio towers and antennas), and antennas typically have a limited bandwidth. Ambient light backscattering not only allows exploiting a different part of the electromagnetic spectrum but it can also exploit *natural* sunlight.

7 Conclusion

In this work, we propose an optical model to analyze ambient light communication, and based on the insights it provides, we explore the use of a DMD as an optical transmitter. We propose a novel platform that optimizes the retention of the luminous flux to attain the best optical performance. This approach allows us to achieve a data rate that is 30 times higher compared to LCs under the same working conditions. Furthermore, with optimally designed receivers, the data rate reaches 80 kbps. While current DMD designs still face limitations to operate with ambient light, it is a component that expands the possibilities of the nascent area of Passive-VLC.

Acknowledgments

References

[1] Dinesh Bharadia, Kiran Raj Joshi, Manikanta Kotaru, and Sachin Katti. Backfi: High throughput wifi backscatter. volume 45, page 283–296, New York, NY, USA, aug 2015. Association for Computing Machinery.

[2] Roy Blokker. Communication with ambient light using digital micromirror devices. Master's thesis, Delft University of Technology, 2021.

[3] Rens Bloom, Marco Zúñiga Zamalloa, and Chaitra Pai. Luxlink: Creating a wireless link from ambient light. In *Proceedings of the 17th Conference on Embedded Networked Sensor Systems*, SenSys '19, page 166–178, New York, NY, USA, 2019. Association for Computing Machinery.

[4] Rens Bloom, Marco Zuniga, Qing Wang, and Domenico Giustiniano. Tweeting with sunlight: Encoding data on mobile objects. In *IEEE INFOCOM 2019 - IEEE Conference on Computer Communications*, pages 1324–1332, 2019.

[5] Cisco. Cisco annual internet report - cisco annual internet report (2018–2023) white paper.

[6] Dana Dudley, Walter Duncan, and John Slaughter. Emerging digital micromirror device (dmd) applications.

[7] Seyed Keyarash Ghiasi, Marco A. Zúñiga Zamalloa, and Koen Langendoen. A principled design for passive light communication. In *Proceedings of the 27th Annual International Conference on Mobile Computing and Networking*, MobiCom '21, page 121–133, New York, NY, USA, 2021. Association for Computing Machinery.

[8] Tilahun Zerihun Gutema, Harald Haas, and Wasiu O. Popoola. Bias point optimisation in lifi for capacity enhancement. *Journal of Lightwave Technology*, 39(15):5021–5027, 2021.

[9] Texas Instrument. Dlp2000 (.2 nhd) dmd datasheet, 2019. https://www.ti.com/lit/ds/symlink/dlp2000.pdf.

[10] Motoi Kodama and Shinichiro Haruyama. Visible light communication using two different polarized dmd projectors for seamless location services. In *Proceedings of the Fifth International Conference on Network, Communication and Computing*, ICNCC '16, page 272–276, New York, NY, USA, 2016. Association for Computing Machinery.

[11] Motoi Kodama and Shinichiro Haruyama. Pulse width modulated visible light communication using digital micro-mirror device projector for voice information guidance system. In *2019 IEEE 9th Annual Computing and Communication Workshop and Conference (CCWC)*, pages 0793–0799, 2019.

[12] Benjamin Lee. Introduction to ±12 degree orthogonal digital micromirror devices (dmds), 2018. https://www.ti.com/lit/an/dlpa008b/dlpa008b.pdf.

[13] Jiangtao Li, Angli Liu, Guobin Shen, Liqun Li, Chao Sun, and Feng Zhao. *Retro-VLC*: Enabling battery-free duplex visible light communication for mobile and iot applications. In Justin Manweiler and Romit Roy Choudhury, editors, *Proceedings of the 16th International Workshop on Mobile Computing Systems and Applications, HotMobile 2015, Santa Fe, NM, USA, February 12-13, 2015*, pages 21–26. ACM, 2015.

[14] Vincent Liu, Aaron Parks, Vamsi Talla, Shyamnath Gollakota, David Wetherall, and Joshua R. Smith. Ambient backscatter: Wireless communication out of thin air. *SIGCOMM Comput. Commun. Rev.*, 43(4):39–50, aug 2013.

[15] Francisco J. Lopez-Hernandez, Rafael Perez-Jiminez, and Asuncion Santamaria. Ray-tracing algorithms for fast calculation of the channel impulse response on diffuse IR wireless indoor channels. *Optical Engineering*, 39:2775–2780, October 2000.

[16] Farshad Miramirkhani and Murat Uysal. Channel modeling and characterization for visible light communications. *IEEE Photonics Journal*, 7(6):1–16, 2015.

[17] Pamela Rae Patterson, Dooyoung Hah, Makoto Fujino, Wibool Piyawattanametha, and Ming C. Wu. Scanning micromirrors: an overview. In Yoshitada Katagiri, editor, *Optomechatronic Micro/Nano Components, Devices, and Systems*, volume 5604, pages 195 – 207. International Society for Optics and Photonics, SPIE, 2004.

[18] Yury Petrov. Optometrika, howpublished = https://github.com/caiuspetronius/optometrika, 2014.

[19] Bui Tuong Phong. Illumination for computer generated pictures. *Commun. ACM*, 18(6):311–317, June 1975.

[20] PureLiFi. http://purelifi.com/, 2021.

[21] A.M. Ramirez-Aguilera, J.M. Luna-Rivera, V. Guerra, J. Rabadan, R. Perez-Jimenez, and F.J. Lopez-Hernandez. A review of indoor channel modeling techniques for visible light communications. In *2018 IEEE 10th Latin-American Conference on Communications (LATINCOM)*, pages 1–6, 2018.

[22] Yu-Xuan Ren, Rong-De Lu, and Lei Gong. Tailoring light with a digital micromirror device. *Annalen der Physik*, 527(7-8):447–470, 2015.

[23] Nils Ole Tippenhauer, Domenico Giustiniano, and Stefan Mangold. Toys communicating with leds: Enabling toy cars interaction. In *2012 IEEE Consumer Communications and Networking Conference (CCNC)*, pages 48–49, 2012.

[24] Nguyen Van Huynh, Dinh Thai Hoang, Xiao Lu, Dusit Niyato, Ping Wang, and Dong In Kim. Ambient backscatter communications: A contemporary survey. *IEEE Communications Surveys Tutorials*, 20(4):2889–2922, 2018.

[25] Purui Wang, Lilei Feng, Guojun Chen, Chenren Xu, Yue Wu, Kenuo Xu, Guobin Shen, Kuntai Du, Gang Huang, and Xuanzhe Liu. Renovating road signs for infrastructure-to-vehicle networking: A visible light backscatter communication and networking approach. In *Proceedings of the 26th Annual International Conference on Mobile Computing and Networking*, MobiCom '20, New York, NY, USA, 2020. Association for Computing Machinery.

[26] Zixiong Wang, Dobroslav Tsonev, Stefan Videv, and Harald Haas. On the design of a solar-panel receiver for optical wireless communications with simultaneous energy harvesting. *IEEE Journal on Selected Areas in Communications*, 33(8):1612–1623, 2015.

[27] Maury Wright. Philips lighting deploys led-based indoor positioning in carrefou, 2015. https://goo.gl/a0tGIj.

[28] Yue Wu, Purui Wang, Kenuo Xu, Lilei Feng, and Chenren Xu. Turboboosting visible light backscatter communication. In *Proceedings of the Annual Conference of the ACM Special Interest Group on Data Communication on the Applications, Technologies, Architectures, and Protocols for Computer Communication*, SIGCOMM '20, page 186–197, New York, NY, USA, 2020. Association for Computing Machinery.

[29] Xieyang Xu, Yang Shen, Junrui Yang, Chenren Xu, Guobin Shen, Guojun Chen, and Yunzhe Ni. Passivevlc: Enabling practical visible light backscatter communication for battery-free iot applications. In *Proceedings of the 23rd Annual International Conference on Mobile Computing and Networking*, MobiCom '17, page 180–192, New York, NY, USA, 2017. Association for Computing Machinery.

[30] Zhice Yang, Zeyu Wang, Jiansong Zhang, Chenyu Huang, and Qian Zhang. Wearables can afford: Lightweight indoor positioning with visible light. In *Proceedings of the 13th Annual International Conference on Mobile Systems, Applications, and Services*, MobiSys '15, page 317–330, New York, NY, USA, 2015. Association for Computing Machinery.